# Observation and Quantification of Aerosol Outflow from Southern Africa Using Spaceborne Lidar


## Abstract

Biomass burning in Africa provides a prolific source of aerosols that are transported from the source region to distant areas, as far away as South America and Australia. Models have long predicted the primary outflow and transport routes. Over time, field studies have validated the basic production and dynamics that underlie these transport patterns. In more recent years, the advancement of spaceborne active remote sensing techniques has allowed for more detailed verification of the models and, importantly, verification of the vertical distribution of the aerosols in the transport regions, particularly with respect to westerly transport over the Atlantic Ocean. The Cloud-Aerosol Transport System (CATS) lidar on the International Space Station has detection sensitivity that provides observations that support long-held theories of aerosol transport from the African subcontinent over the remote Indian Ocean and as far downstream as Australia.


**Significance:**

- Biomass burning in Africa can have impacts as far away as Australia
- Flow of aerosols from Africa towards Australia have long been postulated by transport models, but have been poorly characterized due to lack of measurements
- The CATS instrument on the ISS has detection sensitivity that captures aerosol transport from Africa over the Indian Ocean to Australia

## 1 Introduction

The African continent is a prolific source of aerosols flowing out over the Atlantic and Indian Oceans. Transport of Saharan dust off the continent and over the equatorial and North Atlantic Ocean is well documented.[1-4] It is now appreciated that dust from the African subcontinent, following that transport route, finds its way to the Caribbean and Amazon basins.[5-10] Similarly, evidence of sub-Saharan aerosol and trace gas transports comprised of biomass burning

smoke, dust, and industrial emissions has been documented. These transports fall into three general categories: 1) out over the Atlantic Ocean (originating primarily in tropical Africa north of 20ºS)[11-18]; 2) air mass recirculation from and over the southern portion of the subcontinent[19-21]; and 3) westerly transport out over the Indian Ocean (south of 20ºS).[13-14,18,22-33] The transports and their emission sources mentioned above that contribute to the atmospheric aerosol loading over and off of southern Africa exhibit a strong seasonality and tend to migrate from western tropical southern Africa in May to southeastern southern Africa and Mozambique (September and October).

The Southern African Fire-Atmosphere Research Initiative and Southern African Regional Science Initiative (SAFARI-92 and SAFARI-2000, respectively) were extensive field campaigns specifically designed to study the postulated aerosol and trace gas transports of combined emissions, in general, and biomass burning emissions, in particular, from the southern regions of the African continent.[31,34] While SAFARI 2000 focused on aerosol emissions and transports, it did so primarily over and very near the southern African subcontinent. Easterly and westerly atmospheric transports from southern Africa occurs over expansive areas of the remote Atlantic and Indian Ocean where ground-based and sea surface measurements are sparse and airborne measurements are challenging to obtain. Understanding, following, and documenting atmospheric features such as these requires the use of atmospheric models and satellite data.

Near source regions, aerosol concentrations in outflows are dense and sufficiently optically thick to be rather easily detected by spaceborne passive sensors such as the Moderate Resolution Imaging Spectrometer (MODIS).[35-37] Although optically thick layers can be detected by MODIS or other passive sensors, over ocean the aerosol optical depth cannot be accurately retrieved from MODIS for aerosol layers having aerosol optical depth <0.03.[36,37]

For less optically thick outflows, active remote sensors, such as the Cloud-Aerosol Lidar and Infrared Pathfinder Satellite Observation (CALIPSO)[38] lidar, can be used to detect aerosol layers. However, CALIPSO also requires a minimum density of scatterers before an aerosol layer can be detected. A challenge to both passive and active sensors, as noted by Edwards[39] is that high aerosol concentrations generally do not extend far from the source region. Far from the source region the aerosol is lofted and transported over the Indian Ocean, the aerosol plume spreads (somewhat in the horizontal, but more in the vertical), and thus becomes too diffuse for spaceborne sensors to detect. This is in contrast to the easterly flow out over the

Atlantic, which either occurs within the boundary layer, particularly over Namibia during offshore transport of surface dust,[40] or is bounded between 800 and 500 hPa.[41]

Although transport models routinely predict aerosol plumes over Australia, measurements verifying the plume height and distribution are extremely limited. Some ground-based measurements from Australia have shown evidence of the outflow plume[26,28] but spaceborne measurements that can conclusively track the outflow from the source region to the Australian continent have been lacking. There were initial spaceborne lidar measurements made by the Laser In-space Technology Experiment (LITE)[42] that appear to capture a feature similar to those described in this paper during September 1994. As LITE was a technology demonstration onboard the Space Shuttle, those measurements were limited in coverage and, moreover, the 1064 nm data from LITE was never calibrated. This paper presents, for the first time, calibrated 1064 nm observations that support long-held (>25 years) postulated understandings of atmospheric transport modes from the biomass burning region of subequatorial Africa out over the Indian Ocean and towards Australia.

## 2 The Cloud-Aerosol Transport System (CATS)

There have been only two in-space lidar sensors that have operated over multiple years to capture seasonal transport patterns: CALIPSO and the Cloud-Aerosol Transport System (CATS) onboard the International Space Station (ISS). The CATS sensor is a backscatter lidar instrument with depolarization measurement.[43] A notable feature of CATS is the use of photon-counting detection, which permits high detection sensitivity. As a result, at least during night portions of each orbit, CATS has detection sensitivity (minimum detectable backscatter, at 1064 nm) as low as $5 \times 10^{-5}$ $km^{-1}$ $sr^{-1}$, which is more sensitive than the CALIPSO minimum detection sensitivity (at 532 nm) of ~$8 \times 10^{-4}$ $km^{-1}$ $sr^{-1}$.[44] As noted in the previous section, although the LITE demonstration had detection sensitivity sufficient to detect diffuse aerosol layers, the limited lifetime (approximately 40 hours total observation time) and the limited number of observations over the study region precludes an ability to track individual events as they vary with synoptic conditions. The more continuous and multi-year operation of CATS, coupled with the high detection sensitivity, can be used to demonstrate persistence of the aerosol outflow as well as tracking of the outflow from Africa towards Australia.

Operating from February 2015 until October 2017, CATS data contains observations of each of the outflow patterns identified in Garstang et al.[13] The most intriguing are observations of the westerly transport of aerosols out over the Indian Ocean and over Australia. The detection sensitivity of CATS at 1064 nm has enabled observations of the diffuse aerosol plumes transported off the African subcontinent over those regions, providing direct measurement of the transport predicted by Garstang et al.[13] Moreover, unlike other spaceborne lidar sensors, the CATS 1064 nm data is directly calibrated at 1064 nm[44,45] thereby augmenting the available data record with additional wavelength information.

In addition to backscatter detection, the CATS 1064 nm channel provides a linear depolarization measurement. The depolarization measurement is exceptionally useful as an aid in determining cloud and aerosol type.[46,47] Relevant to African aerosol transport, where smoke and dust (and combinations of the two) are prevalent, the depolarization ratio provides a critical determinant of aerosol type. Smoke tends to have linear depolarization ratio on the order of 1-10%, whereas dust is in the range of 20-30%. Smoke combined with dust will lower the ratio somewhat, typically in the 10-25% range. The depolarization measurement provides important substantiation that the elevated layers observed are, in fact, comprised of smoke particles and, hence, are coming from the expected source region. The LITE demonstration did not have depolarization measurement capability hence making those prior measurements more challenging to relate to aerosol type.

## 3 CATS observations of westerly outflow

The CATS lidar onboard the ISS, with its unique precessing orbit, has captured multiple occurrences of westerly outflow from the African subcontinent towards Australia. The CATS data used herein are calibrated Level 1B (L1B) data products, specifically 1064 nm attenuated total backscatter coefficients at a resolution of 350 m horizontal by 60 m vertical.[44] Three specific examples are described below.

### 3.1 Case 1, 07 September 2016

On 07 September 2016, multiple ISS passes on same day provide a unique Eulerian perspective with multiple snapshots of the resultant transport plume. As illustrated in Figure 1, data captured on subsequent orbits show evolution of an aerosol plume originating off the west coast of southern Africa (approx. latitude 25˚S) and propagating across the Indian Ocean to

south of Australia. Analysis of five-day back trajectories, shown in Figure 2(a), obtained from the Hysplit model[48] indicates that parcels observed in the 9-km altitude range to the west of Australia on 07 September 2016 originated over the west coast of southern Africa (within the free troposphere) as well as from South America. Both these regions are large biomass burning source regions during the austral spring. The trajectory analysis illustrates how transport from the two continents merges in a transient westerly wave over southern Africa and exits the African subcontinent towards the southeast, south of the semi-permanent Indian anticyclone (Figure 3). In this transport pathway air parcels rise rapidly and within two days are separated from the surface layer to become a clearly defined lofted layer. This is consistent with the postulated expectations based on modeled outputs (e.g., Garstang et al[13], Tyson and D'Abreton[20]) that the westerly plumes exiting the subcontinent in a westerly wave tend to ascend over the southern Indian Ocean facilitating rapid transport toward Australasia.

Back trajectory analysis suggests the layer should be in the 9 km altitude range near Australia, and CATS profiles show the layer extending from about 3 km altitude up to about 11 km. This range in the vertical distribution is consistent with what Wenig et al[30] found in the long range transport of nitrogen dioxide plumes between southern Africa and Australia. Such transport is also consistent with previously described transports of water vapor,[49] trace gases,[50] and aerosols[51] off the subcontinent and are transports that have been demonstrated to impact atmospheric chemistry and composition as well as possibly the biogeochemical cycling of precipitation and the ocean surface along the path of transport.[52] Figure 4 shows a cross-section of the elevated plume as it approaches the west coast of Australia. As seen in Figure 4b, the elevated layer is distinct and extends from 3 km up to about 11 km, but with low backscatter of $<5 \times 10^{-4}$ $km^{-1}$ $sr^{-1}$. Although covering a large vertical extent, the median optical depth of the layer west of Australia is only on the order of 0.03 – 0.05 (+/- 0.008). The median depolarization ratio (integrated through the layer) is 0.05 – 0.08, indicating the elevated layer is comprised primarily of smoke. The layer does start with higher optical depth (mean optical depth of 0.15 +/- 0.05) over the African subcontinent which is attenuated as it is transported across the Indian Ocean through the loss of particles by wet and dry removal processes.[25]

### 3.2 Case 2, 11-18 October 2015

In contrast to the Eulerian view of Case 1, over the 8 day period of 11-18 October 2015, CATS captured a Lagrangian view of the evolution and transport of multiple plumes. Data captured during this period, displayed in Figure 5, show evolution of multiple dust/aerosol plumes that

originate over southern Africa (approx. latitude 25˚S) and propagate across the Indian Ocean to the south of Australia. Back trajectory analysis (Figure 2b) again indicates that 5-6 days are required for a plume to transit to Australia. Back trajectory analysis suggests that near the west coast of Australia the layer should be in the 3 km altitude range, and CATS profiles show the layer extending from about 1 km altitude up to about 8 km. The median optical depth of the layer west of Australia is on the order of 0.01 – 0.03 (+/- 0.09). The median depolarization ratio (integrated through the layer) is 0.05 – 0.10, again indicating primarily smoke.

### 3.3 Case 3, 13-19 September 2016

Similar to Case 2, this example presents a Lagrangian view of a plume transiting off southern Africa towards Australia. Figure 6 shows data captured during the period 13-19 September 2016, highlighting the evolution of a plume that transits directly over Australia and then continues on to the south. Similar to the other two cases, back trajectory analysis (Figure 2c) again indicates that 5-6 days are required for the plume to transit to Australia. Back trajectory analysis suggests the layer should be in the 5-6 km altitude range, and CATS profiles show the layer extending from as low as 1 km altitude up to as high as 10 km. Although covering a large vertical extent, the median optical depth of the layer over Australia is low, only on the order of 0.008 – 0.01 (+/- 0.003) and again becoming progressively lower the farther east the plume travels. The median depolarization ratio (integrated through the layer) is 0.02 – 0.08, once again indicating that the layer is comprised primarily of smoke.

### 3.4 Supporting meteorological information

Garstang et al[13] showed that during the dry season in southern Africa (April through October), the dominating synoptic weather pattern is an anticyclonic circulation that results in horizontal recirculation at spatial scales as high as thousands of kilometers. Aerosols exit this anticyclonic flow in the southernmost part of Africa to the east into the Indian Ocean via westerly wave and trough disturbances. These westerly disturbances peak in the spring months (September-November) and in very dry seasons such as observed during the SAFARI project in 1992, can direct as much as 90% of aerosol transport into the Indian Ocean.[13]

Synoptic weather maps of surface pressure and wind from the South African Weather Service were analyzed for the three cases of smoke transport into the Indian Ocean observed by CATS. All three of these cases strongly support the observations during SAFARI-92. Low pressure systems propagating across the southern edge of Africa, in tandem with high pressure located

near Madagascar, result in flow towards the south and east that transport smoke into the Indian Ocean across 35˚E. During this transport, the smoke is lofted and advected toward Australia in the prevailing westerlies at southern latitudes higher than 30˚S. The global atmospheric circulation patterns were also similar between SAFARI-92 and the CATS cases in 2015 and 2016. The National Oceanographic and Atmospheric Administration (NOAA) Oceanic Nino Index (ONI), a rolling 3-month average of sea surface temperatures in the eastern tropical Pacific, indicates relatively strong El Nino conditions existed in 2015 and continued into most of 2016.

Back trajectories obtained from the Hysplit model confirm that transport from Africa to Australia generally took between 5-7 days. The back trajectories were initialized using the centroid of the elevated plume. In Cases 2 and 3, the trajectories trace back to the east coast of southern Africa (near the southern tip of Madagascar) whereas in Case 1 the trajectories trace to the west coast of southern Africa.

## 4 Conclusions

Biomass burning in Africa has long been recognized as a significantly important source of aerosols and trace gas. Focused field studies, such as SAFARI-92 and SAFARI 2000, validated the primary source and outflow patterns for smoke and trace gases from the African subcontinent. The primary outflow and transport routes from Africa to the Atlantic Ocean and over to South America, and from Africa to the Indian Ocean and Australia, have long been predicted via models.

While measurements of a number of these transports have been captured at least spatially and temporally, it was not until the advent of spaceborne active remote sensing by lidar that characterization of these transports in the vertical became possible. Even with spaceborne sensors, detection of aerosol plumes can only be accomplished if the aerosol concentration is sufficient to meet minimum detection thresholds. An aerosol layer that is dense and easily detectable near the source region eventually spreads and disperses beyond the minimum detectable limit for the sensor.

Hence, discerning information on aerosol and trace gas transports has been heavily reliant upon modeled information which is itself suspect in such a data-limited part of the world as the African continent and remote Indian Ocean. The CATS lidar on the ISS had detection sensitivity sufficient to identify diffuse elevated aerosol plumes originating on the African subcontinent and transported towards Australia. As a result, CATS has provided an opportunity to test and validate long-held assumptions regarding the nature of aerosol and trace gas transports in these remote regions of the world.

## Data Availability

The CATS data used in this paper are archived in NASA's Atmospheric Science Data Center (ASDC) Distributed Active Archive Center (DAAC), accessible via the CATS website (https://cats.gsfc.nasa.gov).

## References


1. Carlson, T.N., and Prospero, J.M. (1972). The large scale movement of Saharan air outbreaks over the northern equatorial Atlantic. Journal of Applied Meteorology, 11, 283–297.

2. Talbot, R.W., Harriss, R.C., Browell, E.V., Gregory, G.L., Sebacher, D.I., and Beck, S.M. (1986). Distribution and geochemistry of aerosols in the tropical north Atlantic troposphere: Relationship to Saharan dust. Journal of Geophysical Research, 91(D4), 5173–5182. https://doi.org/10.1029/JD091iD04p05173

3. Swap, R., Ulanski, S., Cobbett, M., and Garstang, M. (1996a). Temporal and spatial characteristics of Saharan dust outbreaks. Journal of Geophysical Research, 101(D2), 4205–4220. https://doi.org/10.1029/95JD03236

4. Husar, R.B., Prospero, J.M., and Stowe, L.L. (1997). Characterization of tropospheric aerosols over the oceans with the NOAA Advanced Very High Resolution Radiometer

optical thickness operational product. Journal of Geophysical Research, 102(D14), 16889–16909. https://doi.org/10.1029/96JD04009

5. Prospero, J.M., Glaccum, R.A., and Nees, R.T. (1981). Atmospheric transport of soil dust from Africa to South America. Nature, 289, 570–572. https://doi.org/10.1038/289570a0

6. Talbot, R.W., Andreae, M.O., Berresheim, H., Artaxo, P., Garstang, M., Harriss, R.C., et al. (1990). Aerosol chemistry during the wet season in central Amazonia: The influence of long-range transport. Journal of Geophysical Research, 95(D10), 16955–16969. https://doi.org/10.1029/JD095iD10p16955

7. Swap, R., Garstang, M., Greco, S., Talbot, R., & Kållberg, P. (1992). Saharan dust in the Amazon Basin. Tellus B, 44, 133–149. https://doi.org/10.3402/tellusb.v44i2.15434

8. Kaufman, Y.J. , Koren, I., Remer, L.A., Tanre, D. Ginoux, P., and Fan, S. (2005). Dust transport and deposition observed from the Terra-Moderate Resolution Imaging Spectroradiometer (MODIS) spacecraft over the Atlantic Ocean. Journal of Geophysical Research, 110(D10). https://doi.org/10.1029/2003JD004436

9. Koren, I., Kaufman, Y.J., Washington, R., Todd, M.C., Rudich, Y., Martins, J.V., et al. (2006). The Bodélé depression: a single spot in the Sahara that provides most of the mineral dust to the Amazon forest. Environmental Research Letters, 1, 014005. https://doi.org/10.1088/1748-9326/1/1/014005

10. Yu, H., Chin, M., Yuan, T., Bian, H., Remer, L.A., Prospero, J.M., et al. (2015). The fertilizing role of African dust in the Amazon rainforest: Afirst multiyear assessment based on data from Cloud-Aerosol Lidar and Infrared Pathfinder Satellite Observations. Geophys. Res. Lett., 42, 1984 1991. https://doi.org/10.1002/2015GL063040

11. Parkin, D.W., Phillips, D.R., Sullivan, R.A.L., and Johnson, L. R. (1972). Airborne dust collections down the Atlantic. Quarterly Journal of the Royal Meteorological Society, 98, 798–808. https://doi.org/10.1002/qj.49709841807

12. Fishman, J., Fakhruzzaman, K., Cros, B., and Mganga, D. (1991). Identification of widespread pollution in the Southern Hemisphere deduced from satellite analyses. Science, 252, 1693-1696.

13. Garstang, M., Tyson, P.D., Swap, R., Edwards, M., Kållberg, P., and Lindesay, J.A. (1996). Horizontal and vertical transport of air over southern Africa. Journal of Geophysical Research, 101(D19), 23721–23736. https://doi.org/10.1029/95JD00844

14. Tyson, P.D., Garstang, M., Swap, R., Kållberg, P., and Edwards, M. (1996a). An air transport climatology for subtropical southern Africa. International Journal of Climatology, 16, 265-291.

15. Anderson, B.E., Grant, W.B., Gregory, G.L., Browell, E.V., Collins, J.E., Jr., Sachse, G.W., et al (1996). Aerosols from biomass burning over the tropical South Atlantic region: Distributions and impacts. Journal of Geophysical Research, 101(D19), 24117–24137. https://doi.org/10.1029/96JD00717

16. Browell, E.V., Fenn, M.A., Butler, C.F., Grant, W.B., Clayton, M.B., Fishman, J., et al (1996). Ozone and aerosol distributions and air mass characteristics over the South Atlantic Basin during the burning season. Journal of Geophysical Research, 101(D19), 24043–24068. https://doi.org/10.1029/95JD02536

17. Swap, R., Garstang, M., Macko, S.A., Tyson, P.D., Maenhaut, W., Artaxo, P., et al. (1996b). The long-range transport of southern African aerosols to the tropical South Atlantic. Journal of Geophysical Research, 101(D19), 23777–23791. https://doi.org/10.1029/95JD01049

18. Stohl, A., Eckhardt, S., Forster, C., James, P., and Spichtinger, N. (2002). On the pathways and timescales of intercontinental air pollution transport. Journal of Geophysical Research, 107(D23), 4684. https://doi.org/10.1029/2001JD001396, 2002

19. Tyson, P.D., Garstang, M., and Swap, R. (1996b). Large-Scale Recirculation of Air over Southern Africa. Journal of Applied Meteorology, 35(12), 2218-2236.

20. Tyson, P.D., and D'Abreton, P.A. (1998). Transport and recirculation of aerosols off southern Africa: Macroscale plume structure. Atmospheric Environment, 32, 1511-1524. https://doi.org/10.1016/S1352-2310(97)00392-0

21. Piketh, S.J., Swap, R.J., Anderson, C.A., Freiman, M.T., Zunckel, M., and Held, G. (1999). The Ben Macdhui high altitude trace gas and aerosol transport experiment. South African Journal of Science, 95, 35-43.

22. Rayner, P.J. and Law, R.M. (1995). A comparison of modelled responses to prescribed $CO_2$ sources. CSlRO Australia, Division of Atmospheric Research, Technical Paper No. 36, 82 pp.

23. Herman, J.R., Bhartia, P.K., Torres, O., Hsu, C., Seftor, C., and Celarier, E. (1997). Global distribution of UV-absorbing aerosols from Nimbus 7/TOMS data. Journal of Geophysical Research, 102(D14), 16,911-16,922. https://doi.org/10.1029/96JD03680

24. Sturman, A.S., Tyson, P.D. and D'Abreton, P.C. (1997). Transport of air from Africa and Australia to New Zealand. Journal of the Royal Society of New Zealand, 27, 485--498.

25. Piketh, S.J., Tyson, P.D., Steffan, W. (2000). Aeolian transport from southern Africa and iron fertilisation of marine biota in the south Indian Ocean. South African Journal of Science, 96, 244-246.

26. Rosen, J., Young, S., Laby, J., Kjome, N., & Gras, J. (2000). Springtime aerosol layers in the free troposphere over Australia: Mildura Aerosol Tropospheric Experiment (MATE 98). Journal of Geophysical Research, 105(D14), 17833-17842.

27. Zunckel, M. Robertson, L., Tyson, P.D. and Rodhe, H. (2000). Modelled transport and deposition of sulpher over Southern Africa. Atmospheric Environment, 34, 2797-2808. https://doi.org/10.1016/S1352-2310(99)00495-1

28. Young, S.A., Langenfelds, R.L., and Rosen, J.M. (2001). Observations over Australia of plumes from distant biomass-burning sources using remote sensing and airborne techniques. IGARSS 2001 proceedings: IEEE 2001 International Geoscience and Remote Sensing Symposium: scanning the present and resolving the future, University of New South Wales, Piscataway, NJ, Institute of Electrical and Electronics Engineers, 88-90.

29. Piketh, S.J., Swap, R.J., Maenhaut, W., Annegarn, H.J., Formenti, P. (2003). Chemical evidence of long-range atmospheric transport over southern Africa. Journal of Geophysical Research, 107, D24,4817, ACH7-1 – 7-13.

30. Wenig, M., Spichtinger, N., Stohl, A., Held, G., Beirle, S., Wagner, T., et al. (2003). Intercontinental transport of nitrogen oxide pollution plumes. Atmos. Chem. Phys., 3, 387-393, 2003. https://doi.org/10.5194/acp-3-387-2003

31. Swap, R.J., Annegarn, H.J., Suttles, J.T., King, M.D., Platnick, S., Privette, J.L., et al. (2003). Africa burning: A thematic analysis of the Southern African Regional Science Initiative (SAFARI 2000). Journal of Geophysical Research, 108(D13), 8465. https://doi.org/10.1029/2003JD003747

32. Pak, B.C., Langenfelds, R.L., Young, S.A., Francey, R.J., Meyer, C.P., Kivlighon, L.M., et al. (2003). Measurements of biomass burning influences in the troposphere over southeast Australia during the SAFARI 2000 dry season campaign. Journal of Geophysical Research, 108(D13), 8480. https://doi.org/10.1029/2002JD002343

33. Duflot, V., Royer, P., Chazette, P., Baray,J.-L., Courcoux, Y., and Delmas, R. (2011). Marine and biomass burning aerosols in the southern Indian Ocean: Retrieval of aerosol optical properties from shipborne lidar and Sun photometer measurements. Journal of Geophysical Research, 116, D14312. https://doi.org/10.1029/2011JD015839

34. Lindesay, J.A., Andreae, M.O., Goldammer, J.G., Harris, G., Annegarn, H.J., Garstang, M., et al (1996). International Geosphere Biosphere Programme/International Global Atmospheric Chemistry SAFARI 92 field experiment: Background and overview. Journal of Geophysical Research, 101, 23521–23530.

35. Remer, L.A., Kleidman, R.G., Levy, R.C., Kaufman, Y.J., Tanre, D., Mattoo, S., et al (2008). Global aerosol climatology from the MODIS satellite sensor. Journal of Geophysical Research, 113, D14S07. https://doi.org/10.1029/2007JD009661

36. Levy, R.C., Mattoo, S., Munchak, L.A., Remer, L.A., Sayer, A.M., Patadia, F., et al (2013). The Collection 6 MODIS aerosol products over land and ocean. Atmospheric Measurement Techniques, 6, 2989-3034. https://doi.org/10.5194/amt-6-2989-2013

37. Sayer, A.M., Hsu, N.C., Lee, J., Kim, W.V., and Dutcher, S.T. (2019). Validation, stability, and consistency of MODIS Collection 6.1 and VIIRS version 1 deep blue aerosol data over land. Journal of Geophysical Research, 124(D8), 4658-4688. https://doi.org/10.1029/2018JD029598

38. Winker, D.M., Hunt, W.H., and McGill, M.J. (2007). Initial performance assessment of the CALIOP. Geophysical Research Letters, 34, L19803. https://doi.org/10.1029/2007GL030135

39. Edwards, D.P., Emmons, L.K., Gille, J.C., Chu, A., Attie, J.-L., Giglio, L., et al. (2006). Satellite-observed pollution from Southern Hemisphere biomass burning. Journal of Geophysical Research, 111. https://doi.org/10.1029/2005JD006655

40. Tlhalerwa, K., Freiman, M.T., and Piketh, S.J. (2005). Aerosol deposition off the Southern African West Coast by berg winds. South African Geographical Journal, 87, 152-161. http://doi.org/10.1080/03736245.2005.9713838

41. Adebiyi, A.A., and Zuidema, P. (2016). The role of the southern African easterly jet in modifying the southeast Atlantic aerosol and cloud environments. Quarterly Journal of the Royal Meteorological Society, 142, 1574-1589. http://doi.org/10.1002/qj.2765

42. Kent, G.S., Trepte, C.R., Skeens, K.M., and Winker, D.M. (1998). LITE and SAGE II measurements of aerosols in the southern hemisphere upper troposphere. Journal of Geophysical Research, 103(D15), 19111-19127. https://doi.org/10.1029/98JD00364

43. McGill, M.J., Yorks, J.E., Scott, V.S., Kupchock, A.W., and Selmer, P.A. (2015). The Cloud-Aerosol Transport System (CATS): A technology demonstration on the International Space Station. Proceedings of the SPIE 9612, Lidar Remote Sensing for Environmental Monitoring XV, 96120A. https://doi.org/10.1117/12.2190841

44. Yorks, J.E., McGill, M.J., Palm, S.P., Hlavka, D.L., Selmer, P.A., Nowottnick, E.P., et al. (2016). An overview of the CATS level 1 processing algorithms and data products. Geophysical Research Letters, 43, 4632-4639. https://doi.org/10.1002/2016GL068006

45. Pauly, R.M., Yorks, J.E., Hlavka, D.L., McGill, M.J., Amiridis, V., Palm, S.P., et al. (2019). Cloud-Aerosol Transport System (CATS) 1064 nm calibration and validation. Atmospheric Measurement Techniques, 12, 6241-6258. https://doi.org/10.5194/amt-12-6241-2019

46. Omar, A.H., Winker, D.M., Kittaka, C., Vaughan, M.A., Liu, Z., Hu, Y., et al. (2009). The CALIPSO automated aerosol classification and lidar ratio selection algorithm. Journal of Atmospheric and Oceanic Technology, 26, 1994-2014. https://doi.org/10.1175/2009JTECHA1231.1

47. Groβ, S., Esselborn, M., Weinzierl, B., Wirth, M., Fix, A., and Petzold, A. (2013). Aerosol classification by airborne high spectral resolution lidar observations. Atmospheric Chemistry and Physics, 13, 2487-2505. https://doi.org/10.5194/acp-13-2487-2013

48. Stein, A.F., Draxler, R.R., Rolph, G.D., Stunder, B.J.B., Cohen, M.D., and Ngan, F. (2015). NOAA's Hysplit atmospheric transport and dispersion modeling system. Bulletin of the American Meteorological Society, 96, 2059-2077. https://doi.org/10.1175/BAMS-D-14-00110.1

49. D'Abreton, P.C., and Tyson, P. (1995). Divergent and non-divergent water vapor transport over southern Africa during wet and dry conditions. Meteorology and Atmospheric Physics, 55, 47-59. https://doi.org/10.1007/BF01029601

49. Thompson, A.M., Balashov, N.V., Witte, J.C., Coetzee, J.G.R., Thouret, V., and Posny, F. (2014). Tropospheric ozone increases over the southern Africa region: bellwether for rapid growth in Southern Hemisphere pollution? Atmospheric Chemistry and Physics, 14, 9855-9869. https://doi.org/10.5194/acp-14-9855-2014

50. Piketh, S.J., Annegarn, H.J., and Tyson, P.D. (1999). Lower tropospheric aerosol loadings over South Africa: The relative contribution of aeolian dust, industrial emissions, and biomass burning. Journal of Geophysical Research, 104, 1597-1607. https://doi.org/10.1029/1998JD100014

51. Moody, J.L., Pszenny, A.A.P., Gaudry, A., Keene, W.C., Galloway, J.N., and Polian, G. (1991). Precipitation composition and its variability in the southern Indian Ocean: Amsterdam Island, 1980-1987. Journal of Geophysical Research, 96, 20769-20786. https://doi.org/10.1029/91JD01921

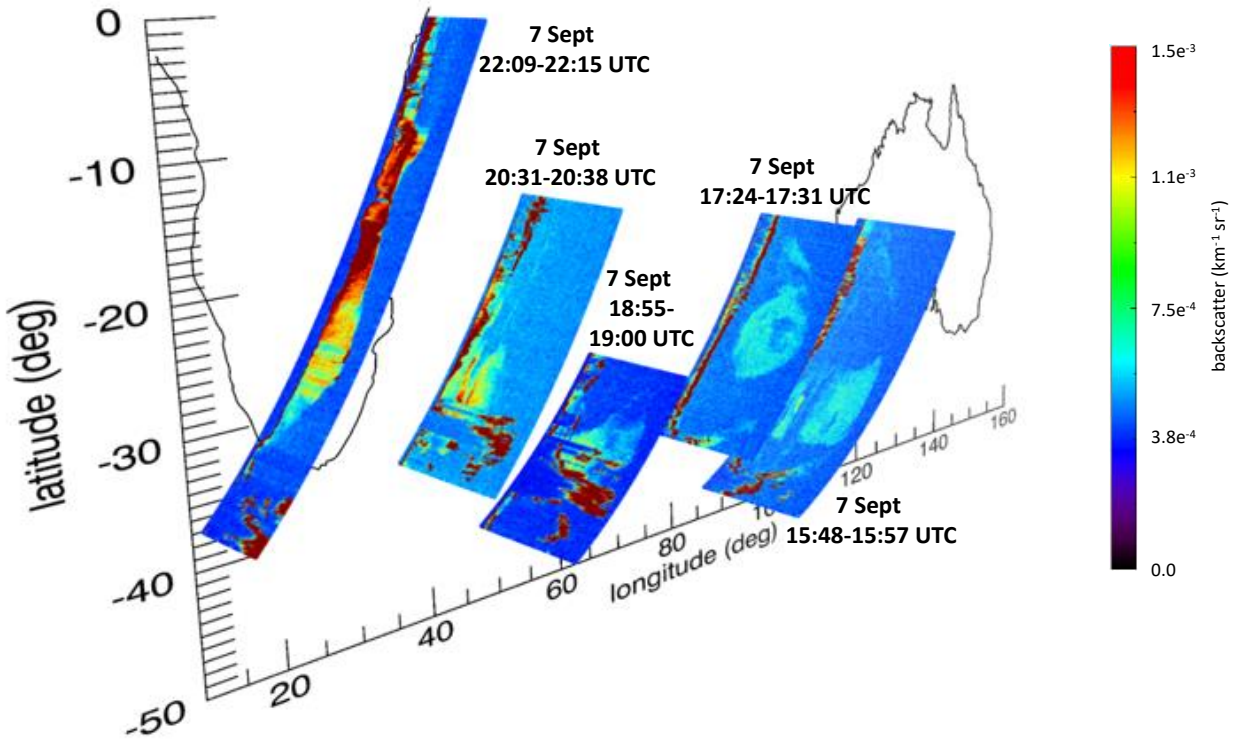


**Figure 1**: Case 1, 07 September 2016, showing an Eulerian view of plume transport. This visualizes cross-sections of plumes on different passes during the same day. Time intervals of each cross-sectional segment are as noted on the image. The elevated plume shows as a light blue color in the images; the dark red/brown color is cloud. The 4th track from the left (7 Sept 17:27 UTC) is further detailed in Figure 3.

a)

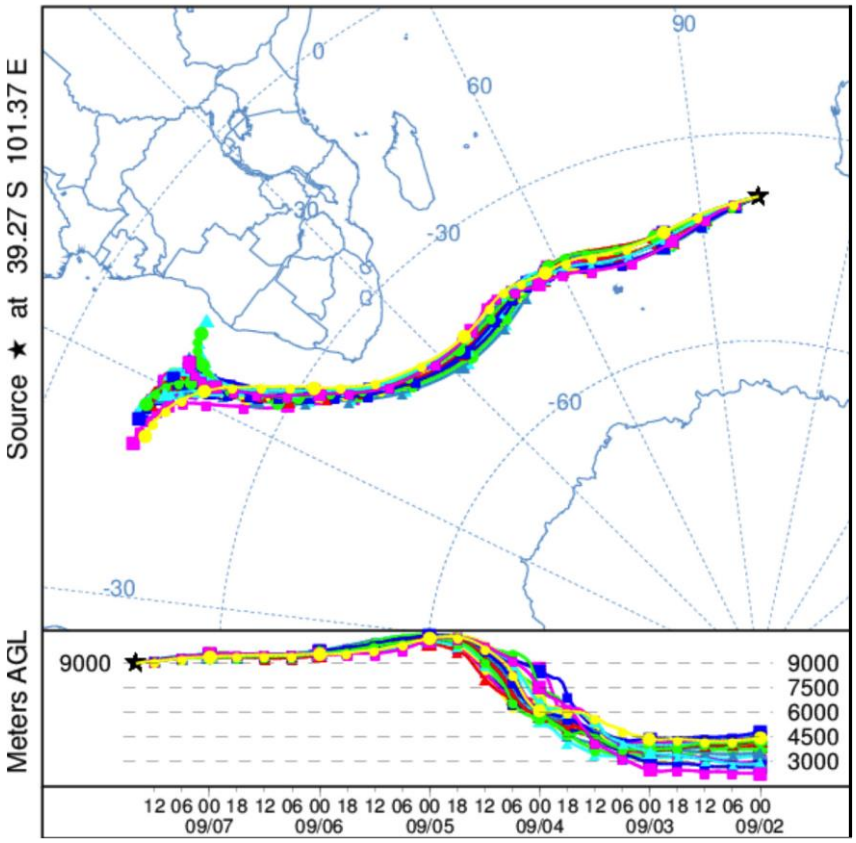
Source ★ at 39.27 S 101.37 E
90
60
30
0
-30
-60
-30
Meters AGL
9000
9000
7500
6000
4500
3000
12 06 00 18 12 06 00 18 12 06 00 18 12 06 00 18 12 06 00 18 12 06 00
09/07 09/06 09/05 09/04 09/03 09/02

b)

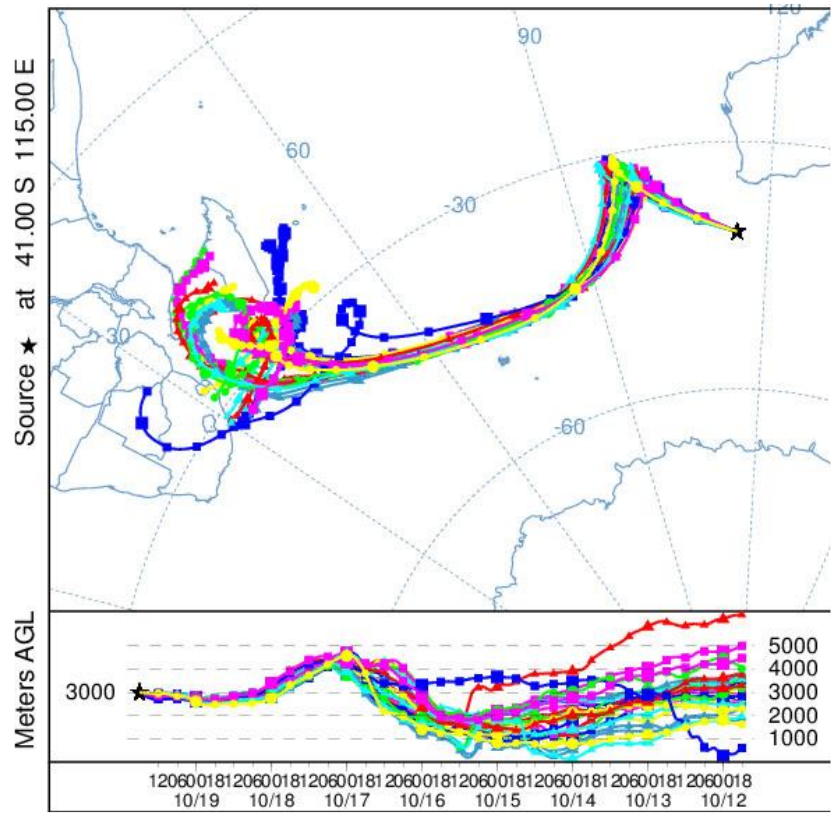
Source ★ at 41.00 S 115.00 E
90
60
30
0
-30
-60
Meters AGL
3000
5000
4000
3000
2000
1000
12060018120600181206001812060018120600181206001812060018120600181206001812060018
10/19 10/18 10/17 10/16 10/15 10/14 10/13 10/12

c)

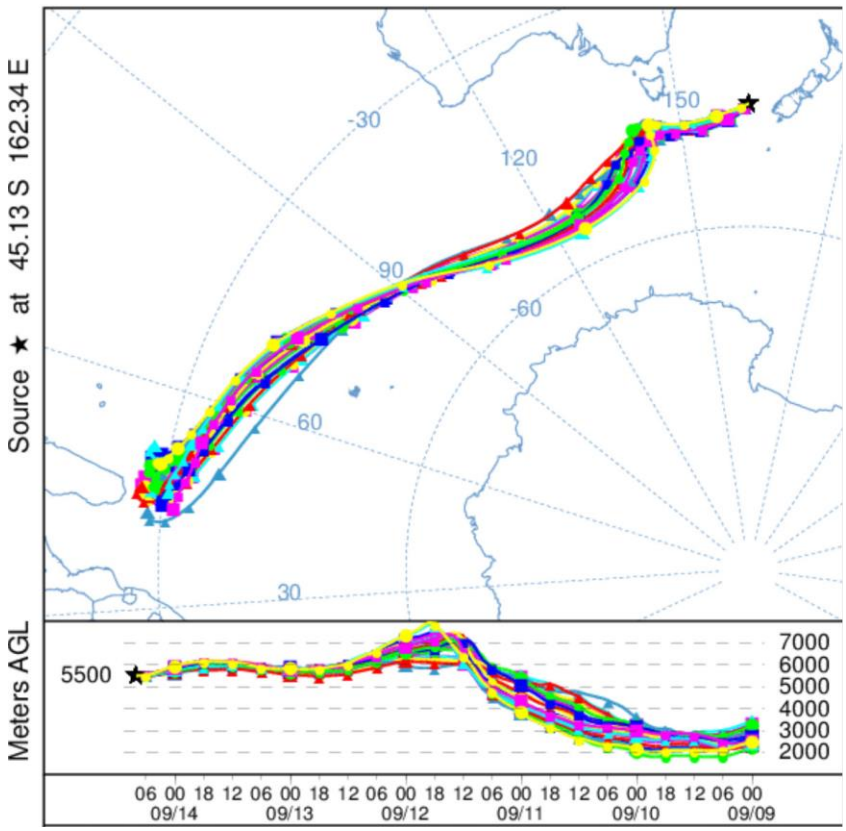


**Figure 2**: Back trajectory analyses from the NOAA Hysplit model. (a) for data shown in Figure 1, 07 September 2016; (b) for data shown in Figure 5, 11-18 October 2015; (c) for data shown in Figure 6, 13-19 September 2016.

# 4 Sept 2016

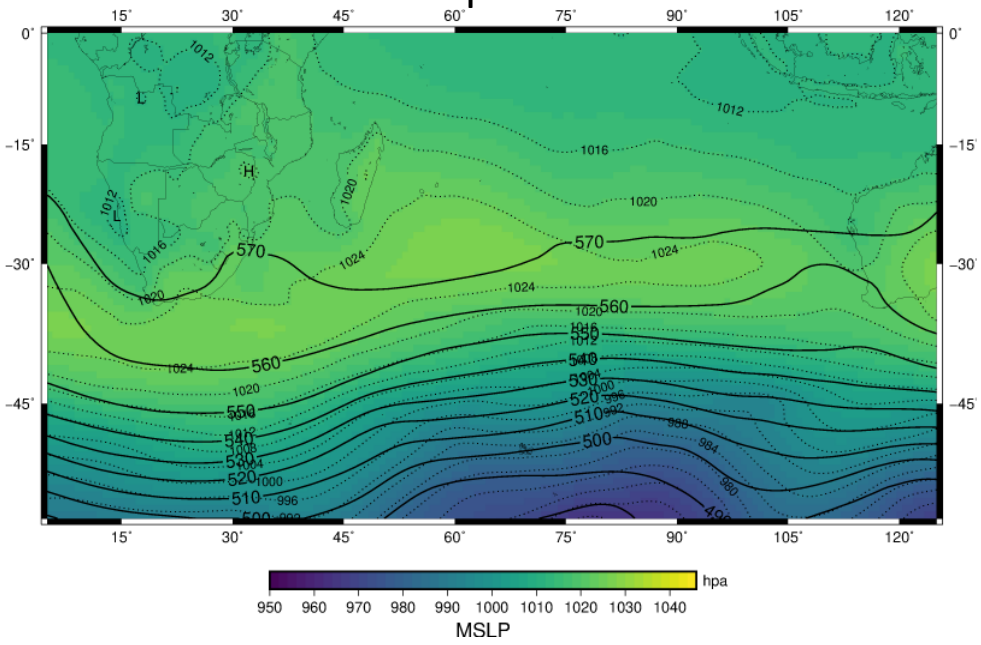


# 5 Sept 2016

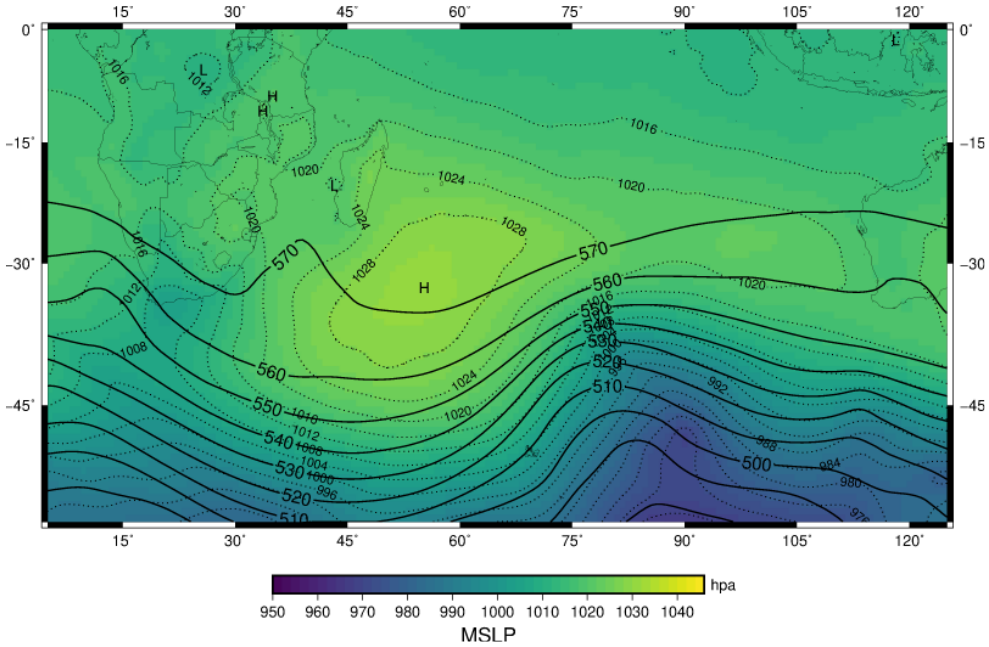

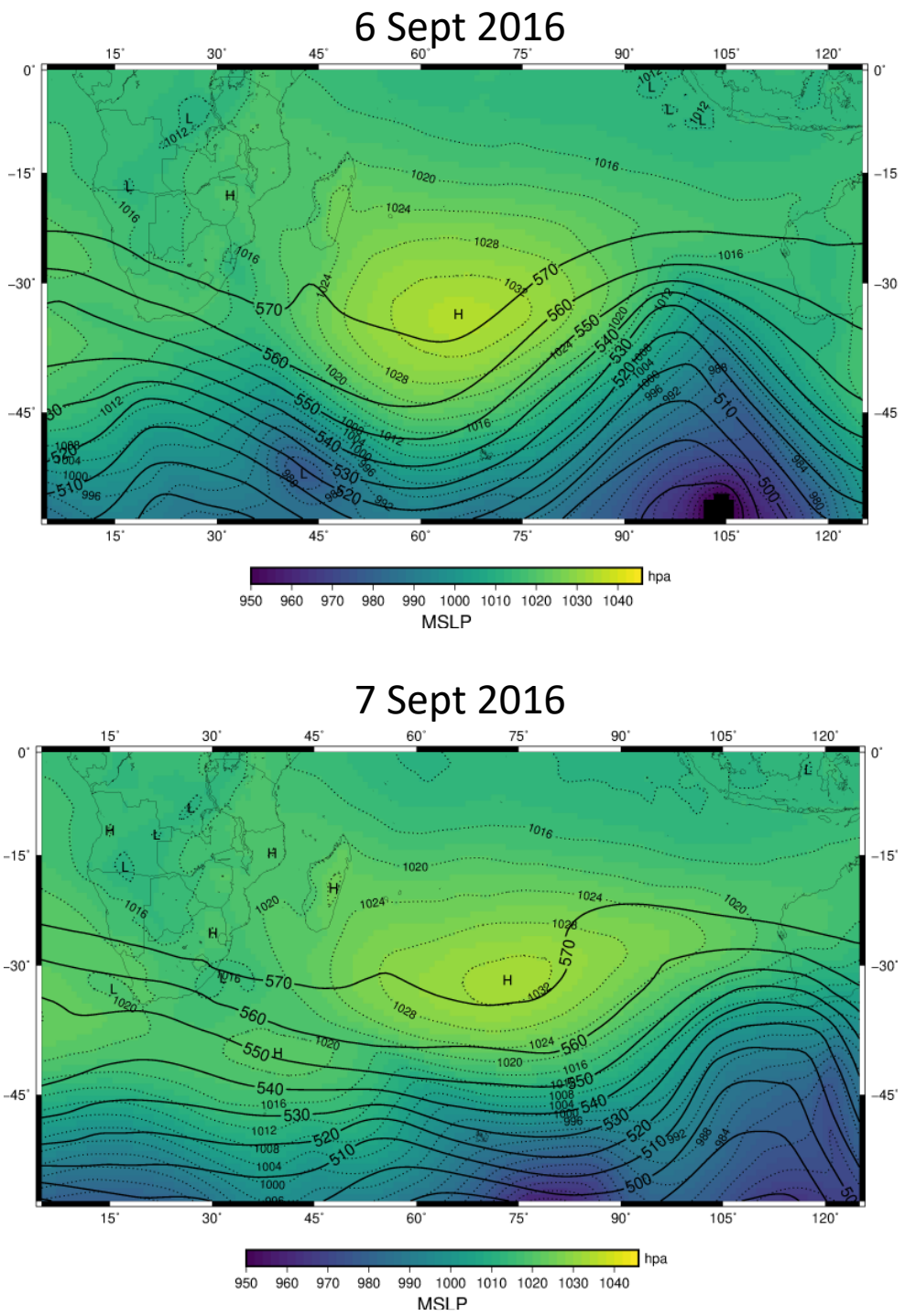


**Figure 3:** ECMWF Reanalysis plots indicating the large scale circulation from southern Africa to Australia for 4-7 September 2016 that coincides with Case 1. The dashed lines indicate the isobars at the surface while the solid lines give the isobars at 500 hPa. The shading is the geopotential height. The transient westerly wave, driving both the rapid atmospheric transport as well as the lofting mechanism, is seen clearly as it moves from the west of southern Africa and transitions to a location over the South Indian ocean.

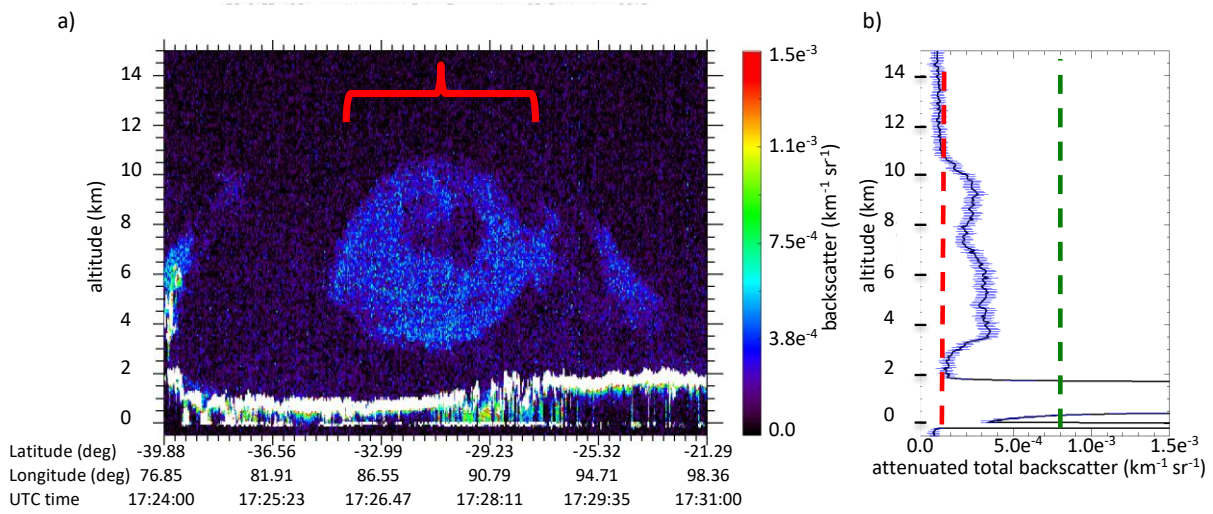


**Figure 4**: a) Cross-section of the backscatter west of Australia on 07 September 2016. The profile on the right (b) is an average of backscatter through the layer (95-second average, as indicated by the red bracket on the figure) to show the structure and low magnitude (< 5 x $10^{-4}$ $km^{-1}$ $sr^{-1}$) of the backscatter. The red dashed line on (b) indicates the CATS minimum detection threshold while the green dashed line indicates same for CALIPSO.

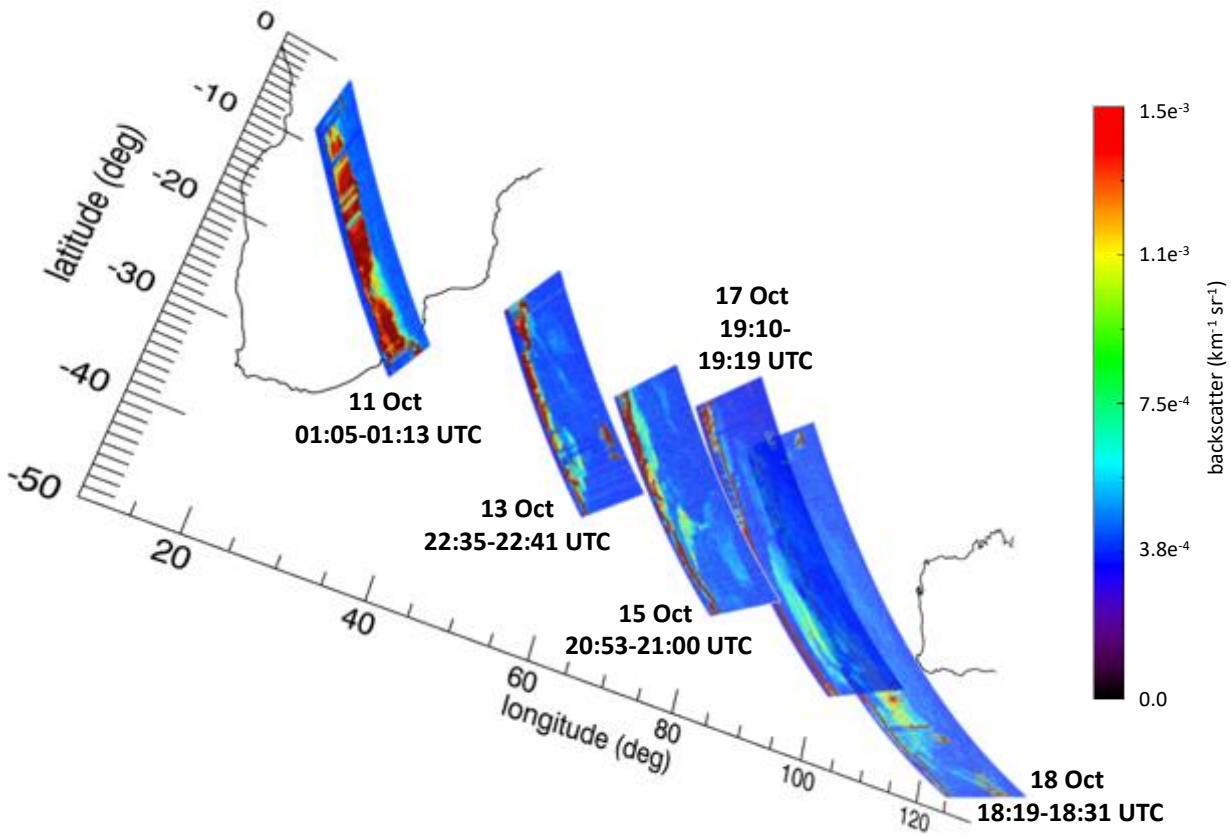


**Figure 5**: Case 2, 11-18 October 2015, demonstrating a Lagrangian view of plume transport, showing different passes on subsequent days. Time intervals of each cross-sectional segment are as noted on the image. The elevated plume shows as light blue color in the images; the dark red/brown color is cloud.

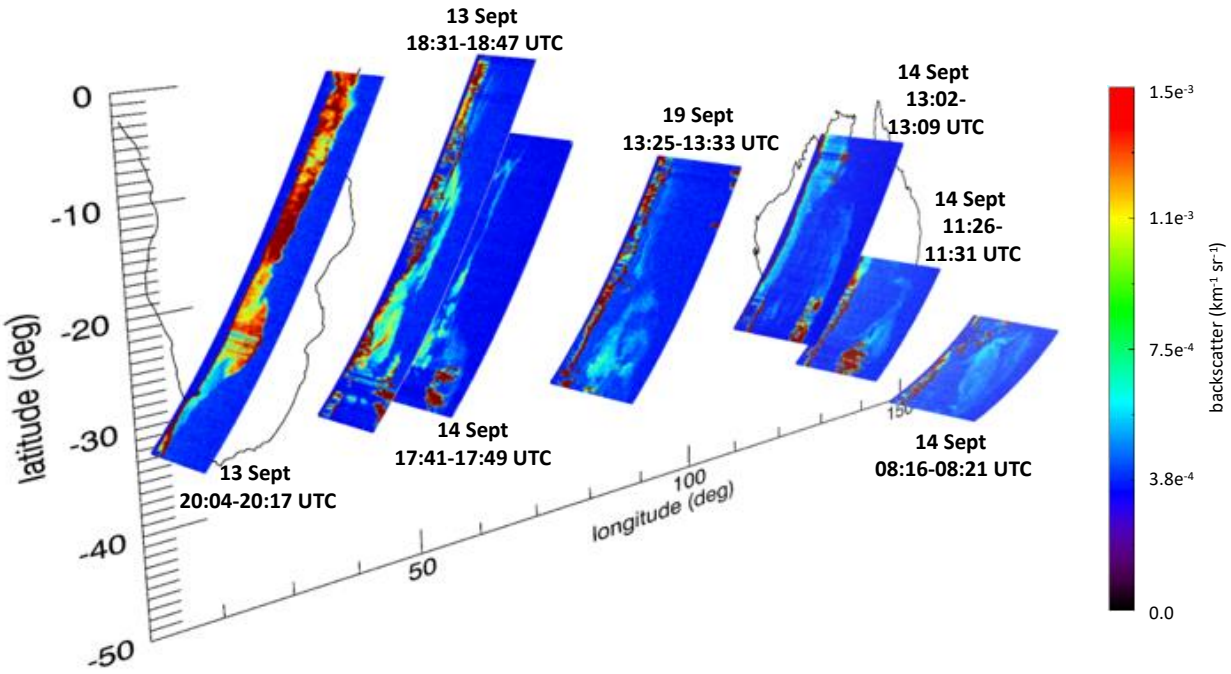


**Figure 6**: Case 3, 13-19 September 2016, demonstrating a Lagrangian view of plume transport, showing different passes on subsequent days. The elevated plume shows as light blue color in the images; the dark red/brown color is cloud.